

Short-range correlations in two-nucleon knockout reactions

C. A. Bertulani*

Department of Physics, University of Arizona, Tucson, Arizona 85721

(Dated: April 18, 2019)

Abstract

The theory of short-range correlations in two-nucleon removal due to elastic breakup (diffraction dissociation) on a light target is developed and compared to previously published works. The main fingerprints of these correlations will appear in momentum distributions of back-to-back emission of the nucleon pair. Expressions for the momentum distributions are derived and calculations for reactions involving stable and unstable nuclear species are performed. The signature of short-range correlations in other reaction processes is also studied.

PACS numbers: 21.10.Jx, 24.50.+g, 25.60.-t, 27.20.+n

Keywords: Knockout reactions, short-range correlations, momentum distributions

arXiv:nucl-th/0504048v1 15 Apr 2005

*Electronic address: bertulani@physics.arizona.edu

I. INTRODUCTION

A primary goal of nucleus-nucleus scattering has been to learn about nuclear structure. This has become even more critical in recent years, when many groups became very active in the investigation of the physics of nuclei far from the stability, mainly using nucleus-nucleus scattering processes at intermediate energies ($E_{lab} \simeq 100$ MeV/nucleon). The complexity of such collisions has given rise to the use of a number of different approximations in the theoretical treatments. The adequate theoretical tool for this purpose is Glauber's multiple-scattering theory [1]. It has long been known both for its simplicity and amazing predictive power. One can find copious examples in the literature where such theory allows for a simple physical interpretation of experimental results as well as their quantitative analysis [2, 3, 4]. In fact, fragmentation reactions of the type discussed here have already been successfully analyzed in the framework of Glauber's theory: in one-nucleon-removal reactions, the momentum distribution of the outgoing fragment has been shown to reflect the momentum distribution of the nucleon which is removed from the surface of the projectile nucleus [3]. However, because of the complicated geometries involved in the multiple scattering that occur in nucleus-nucleus collisions a full Glauber multiple scattering expansion is impracticable. Fortunately, many direct nuclear processes, e.g. nucleon knockout, or stripping, elastic breakup (diffraction dissociation), etc, are possible to study using the optical limit of the Glauber theory, in which the nuclear ground-state densities and the nucleon-nucleon total cross sections are the main input. In fact, this method has become one of the main tools in the study of nuclei far from stability [5]. When departures from the optical limit are observed, multiple nucleon-nucleon collisions and in-medium effects of the nucleon-nucleon interaction and nucleon-nucleon correlations become relevant.

Very peripheral collisions, with impact parameters just around the sum of the nuclear radii (grazing collisions), or larger, are well established tools for studying nuclear properties with intermediate energies and relativistic heavy ion collisions [6, 7, 8]. These collisions lead to excitation of giant resonances through both electromagnetic and strong interactions. At intermediate energy collisions ($E_{lab} \simeq 100$ MeV/nucleon) or higher, the collision time is short and the action of the short-range nuclear interaction can excite the surface region of the colliding nuclei. This excitation can equilibrate forming a compound nucleus, and/or give rise to pre-equilibrium emission or other fast dissipation process.

An interesting reaction mechanism in high-energy peripheral nucleus-nucleus collisions was suggested by Feshbach and Zabek [9, 10]. This mechanism has been applied in refs. [11, 12, 13, 14, 15, 16] to the calculation of pion production in heavy ion collisions from subthreshold to relativistic energies. It is assumed that pions are produced in peripheral processes through the excitation of the projectiles to a Δ -isobar giant resonance. The results of these calculations were compared to inclusive pion production data for incident energies from 50 MeV to 2 GeV per nucleon. As emphasized by those authors, this comparison is not very meaningful at high energy where peripheral processes are expected to contribute very little to the total pion production. However, at subthreshold energies, coherent pion production should dominate the cross section. This mechanism is known as the nuclear Weizsaecker-Williams method. It works as follows.

The uncertainty relation associated to the variation of the time-dependent nuclear field on a scale Δz leads to the energy and momentum of the nuclear interaction pulse in a peripheral collisions as

$$E \simeq \frac{\hbar}{\Delta t} = \frac{\hbar v}{\Delta z}, \quad p \simeq \frac{\hbar}{\Delta z} \quad \implies \quad E = pv.$$

The last equation on the right is the dispersion relation of a phonon. For typical situations, Δz is a few fermis and the nuclear interaction pulse can carry several hundred MeV. This relation can also be directly obtained from the collision kinematics. Let (E_i, \mathbf{p}_i) be the initial momentum of the projectile and (E, \mathbf{p}) the energy-momentum transfer in the reaction. One has

$$\mathbf{P}_f = \mathbf{P}_i - \mathbf{p}, \quad E_f = E_i - E.$$

From these relations one finds

$$\frac{\mathbf{P}_i \cdot \mathbf{p}}{E_i} - E = \frac{-E^2 + p^2 + (M_i^2 - M_f^2) c^4}{2E_i}.$$

We can neglect the term on the right-hand side, obtaining

$$E = \mathbf{v} \cdot \mathbf{p} = vp_z, \tag{1}$$

where p_z is the momentum transfer along the longitudinal direction.

The above relation can only be satisfied for nuclear excitations of very small momentum transfers, even for moderately large energy transfers. This is the case for the excitation of giant resonances. Thus, the nuclear interaction in grazing nuclear collisions is an effective

way to excite giant resonances (for a review see, e.g. ref. [17]). For very large impact parameters (larger than the sum of the nuclear density radii) only the electromagnetic interaction is present, and eq. 1 (with $v \simeq c$) is just the energy-momentum relation of a real photon. In fact, relativistic Coulomb excitation is a useful tool for investigating giant resonances [6, 8].

The phonon-like relation, eq. 1, is also a possible mechanism for studying nucleon-nucleon short-range correlations. This can be seen as follows. The energy in eq. 1 could hardly be absorbed by a single nucleon since it would carry the momentum $\sim \sqrt{2mE}$, which is appreciably larger than that of eq. 1. However, the phonon could be absorbed by a correlated nucleon-pair, which can have high kinetic energy and small total momentum, when the nucleons move along approximately opposite directions. This mechanism has been exploited by previous authors to study the emission of correlated pairs in relativistic heavy ion collisions [20, 21]. Remarkably, refs. [9, 10] do not treat nuclear absorption at small impact parameters properly leading to very large cross sections for the emission of correlated pairs in peripheral collisions.

In many-body physics the word correlation is used to indicate effects beyond mean-field theories. In nuclear physics one distinguishes between short- and long-range correlations. Nuclear collective phenomena such as vibrations and rotations are known to be ruled by long-range correlations. These effects are relatively well known. However, the study of the short-range correlations is a relatively new issue in nuclear physics [18, 19]. The sources of short-range correlations are the strong repulsive core of the microscopic nucleon-nucleon interaction at short internucleon distances. The nucleon-nucleon interaction becomes strongly repulsive at short distances in the relative coordinate of two nuclear particles. The phase shifts for 1S_0 and 3S_1 are positive at low and becomes negative at higher energies [25]. This indicates a repulsive core at short distances and attraction at long distances. In the nuclear medium this repulsive interaction is strongly influenced by Pauli blocking. The search for nuclear phenomena showing short-range correlations effects is one of the most discussed topics in the nuclear structure community. For the nuclear reaction community, the importance of Pauli correlations in high energy nucleus-nucleus collisions has prompted the consideration of effects of dynamical short-range correlations. When one treats nucleus-nucleus collisions at high energies with an optical phase shift function one can include both the center-of-mass correlations and two-body correlations in a straightforward manner to obtain a rapidly converging series for the physical observables.

It would be very proper at this time to look for fingerprints of short-range correlations in nucleus-nucleus collisions at high energies. In particular, because recent experiments on knockout reactions seem to indicate a quenching of the spectroscopic factor relative to shell-model predictions [5]. This reduction is thought to be a consequence of short-range correlations which spread the single particle strength to states with higher energies. In this context, two-proton knockout reactions with exotic nuclear beams seem to be a promising tool to investigate these correlations [22]. The phonon mechanism, proposed by Feshbach and Zabeck, is a useful guide for this investigation.

The plan of this paper is as follows. In this work we treat the effects of short-range correlations on heavy-ion scattering at high energies. In Sec. 2 the Glauber formalism for diffraction dissociation is reviewed. In section 3 this formalism is shown to lead to the same result as the traditional DWBA calculations under the proper conditions. This is an important point, as diffraction dissociation and DWBA approaches are commonly referred to as distinct reaction mechanisms in the literature. In section 4 the role of absorption and Lorentz boosts is discussed. In section 5 the formalism is applied to heavy-ion collisions in the presence of two-body correlations, showing the connection with the Feshbach and Zabeck method. The significance of short-range correlations is further discussed. In sec. 6 the formalism is applied to carbon-carbon and $^{11}\text{Li} + ^9\text{Be}$ collisions. In Sec. 7 some concluding remarks are made.

II. DIFFRACTION DISSOCIATION

Let us consider high energy scattering, so that the energy transfer in the collision, ΔE , is much smaller than the kinetic energy of the colliding nuclei, E . In most cases, one is also interested in processes for which the fragments fly in the forward direction, i.e. we will also assume that $\Delta\theta \ll 1$. In such situations the wavefunction of the particles are well described by eikonal waves [23], i.e. a plane wave distorted by an interaction, V , so that the S -matrix is given by the simple formula $S(b) = \exp\left[-(i/\hbar v) \int dZ V(R)\right]$, with v equal to the projectile velocity and $R = (\mathbf{b}, Z)$ the distance between projectile and target (V is assumed to be spherically symmetric). Extending this approach to account for scattering of particles within the projectile, one obtains the wavefunctions for the initial and final states

as

$$\Psi_i = \phi_i(\mathbf{r}) \exp(i\mathbf{k} \cdot \mathbf{R}), \quad \Psi_f = \phi_f(\mathbf{r}) S(b) \exp(i\mathbf{k} \cdot \mathbf{R}), \quad (2)$$

where $\phi_{i,f}(\mathbf{r})$ are the initial and final probability amplitudes (wavefunctions) that a particle in the projectile is at a distance \mathbf{r} from its center of mass. The particle's S -matrix, $S(b)$, accounts for the distortion due to the interaction.

One can now extend the same procedure to the wavefunctions of a two-body system (e.g. a core+valence particle). This yields the diffraction dissociation formula. The wavefunction of a two-body projectile in the initial and final states is given by

$$\begin{aligned} \Psi_i &= \phi_i(\mathbf{r}) \exp[i(\mathbf{k}_c \cdot \mathbf{r}_c + \mathbf{k}_v \cdot \mathbf{r}_v)] \\ \Psi_f &= \phi_f(\mathbf{r}) S_c(b_c) S_v(b_v) \exp[i(\mathbf{k}'_c \cdot \mathbf{r}_c + \mathbf{k}'_v \cdot \mathbf{r}_v)], \end{aligned} \quad (3)$$

where now $\phi_{i,f}(\mathbf{r})$ are the initial and final intrinsic wavefunctions of the (core+valence particle) as a function of $\mathbf{r} = \mathbf{r}_1 - \mathbf{r}_2$. The relation between the intrinsic, \mathbf{r} , and center of mass, \mathbf{R} , coordinates is given in terms of the mass ratios $\beta_i = m_i/m_P$. Explicitly, $\mathbf{r}_v = \mathbf{R} + \beta_c \mathbf{r}$ and $\mathbf{r}_c = \mathbf{R} - \beta_v \mathbf{r}$. The core and valence particle S -matrices, $S_c(b_c)$ and $S_v(b_v)$, account for the distortion due to the interaction with the target.

The probability amplitude for diffraction dissociation is the overlap between the two wavefunctions above, i.e.

$$A_{(\text{diff})} = \int d^3r_c d^3r_v \phi_f^*(\mathbf{r}) \phi_i(\mathbf{r}) \delta(z_c + z_v) S_c(b_c) S_v(b_v) \exp[i(\mathbf{q}_c \cdot \mathbf{r}_c + \mathbf{q}_v \cdot \mathbf{r}_v)], \quad (4)$$

where $\mathbf{q}_c = \mathbf{k}'_c - \mathbf{k}_c$ is the momentum transfer to the core particle, and accordingly for the valence particle. The above formula yields the probability amplitude that the projectile starts the collision as a bound state and ends up as two separated pieces, in this case, the core and the valence particle (e.g. a proton or a neutron). All the information for the dissociation mechanism comes from the knowledge of the S -matrices, S_c and S_v . The delta-function $\delta(Z)$ was introduced in the eq. 4 to account for the fact that the S -matrices calculated in the eikonal approximation only depend on the transverse direction.

It is instructive to follow another argument to obtain eq. 4. If in the scattering process only the core scatters elastically, whereas the valence particle remains in its unaltered plane wave state, the final projectile wavefunction is given by

$$\Psi_f^{(\text{scatt})} = \phi_f(\mathbf{r}) [1 - S_c(b_c)] \exp[i(\mathbf{k}'_c \cdot \mathbf{r}_c + \mathbf{k}'_v \cdot \mathbf{r}_v)]. \quad (5)$$

The factor $[1 - S_c(b_c)]$ is the amplitude for elastic scattering of the core. The same relation can be applied for the valence particle. The diffraction dissociation occurs by subtracting the simultaneous scattering of the core+valence particle, represented by $[1 - S_c(b_c)][1 - S_v(b_v)]$, from the independent scattering of core and the valence particle, i.e.

$$\widehat{S}_{(\text{diff})} = [1 - S_c(b_c)][1 - S_v(b_v)] - [1 - S_c(b_c)] - [1 - S_v(b_v)] = S_c(b_c) S_v(b_v) - 1. \quad (6)$$

The factor (-1) is not relevant because of the orthogonality of the wavefunctions $\phi_i(\mathbf{r})$ and $\phi_f(\mathbf{r})$. Using $A_{(\text{diff})} = \langle \phi_i \varphi_{\mathbf{k}_1, \mathbf{k}_2} | \widehat{S}_{(\text{diff})} | \phi_f \varphi_{\mathbf{k}'_1, \mathbf{k}'_2} \rangle$, with $\varphi_{\mathbf{k}_1, \mathbf{k}_2}$ equal to plane waves, we regain eq. 4. We thus see that diffractive dissociation (or elastic nuclear breakup) arises from the momentum transfer to each particle due to elastic scattering, minus the momentum transfer to their center of mass.

The cross section for the diffraction process $\phi_i(\mathbf{r}) \rightarrow \phi_f(\mathbf{r})$ is given by

$$d\sigma = \rho(E) \left| \int d^3r_c d^3r_v \phi_f^*(\mathbf{r}) \phi_i(\mathbf{r}) \delta(z_c + z_v) S_c(b_c) S_v(b_v) \exp[i(\mathbf{q}_c \cdot \mathbf{r}_c + \mathbf{q}_v \cdot \mathbf{r}_v)] \right|^2, \quad (7)$$

where $\rho(E)$ is the density of final states, $\rho(E) = \delta(Q_z) d^3q_c d^3q_v / (2\pi)^5$, where $\mathbf{Q} = \mathbf{q}_c + \mathbf{q}_v$ is the momentum transfer to the center of mass of the projectile. The delta function accounts for the conservation of the longitudinal momentum of the projectile arising from the use of eikonal wavefunctions.

It is important to notice that the above formula is somewhat different than eq. 8 of ref. [24]. In that reference the coordinates \mathbf{r}, \mathbf{R} were used from the start. One can transform the integral of eq. 7 to those variables. The Jacobian of the transformation is equal to one and $d^3r_c d^3r_v = d^3r d^3R$, $d^3q_c d^3q_v = d^3q d^3Q$, where $\mathbf{q} = \beta_c \mathbf{q}_v - \beta_v \mathbf{q}_c$ is the momentum transfer to the intrinsic coordinates of the projectile. Thus, in the coordinates \mathbf{r}, \mathbf{R} , eq. 7 reduces to

$$d\sigma = \frac{d^3q d^2Q}{(2\pi)^5} \left| \int d^3r d^2b \phi_f^*(\mathbf{r}) \phi_i(\mathbf{r}) S_c(b_c) S_v(b_v) \exp[i(\mathbf{q} \cdot \mathbf{r} + \mathbf{Q} \cdot \mathbf{b})] \right|^2. \quad (8)$$

The above formula reduces to eq. 8 of ref. [24] if one sets $\beta_v = 1$ and $\beta_c = 0$. In this equation, $\phi_f(\mathbf{r})$ can be taken as any final state of the projectile. Thus, it is not only appropriate to calculate *diffraction dissociation*, but also *diffraction excitation*. Diffraction excitation occurs when the final state $\phi_f(\mathbf{r})$ is a bound state. If it is a state in the continuum (diffraction dissociation), then $\phi_f(\mathbf{r})$ should be set to one, since the part of the wavefunction given by $S_c S_v \exp[i(\mathbf{k}'_c \cdot \mathbf{r}_c + \mathbf{k}'_v \cdot \mathbf{r}_v)]$ already accounts for the wave character of the projectile. A

natural improvement of eq. 7 is to include final state interactions between the core and the valence particle in the coordinate dependence of $\phi_f(\mathbf{r})$.

Since we claim here that eq. 8 can also be used for calculating excitation cross sections, it is adequate to show the relation of this approach to the traditional DWBA and semiclassical methods for nuclear excitation in nucleus-nucleus collisions. We will see that the later are perturbative expansions of the eq. 8.

III. DWBA AND SEMICLASSICAL METHODS

One can factorize the S -matrices defined in section 2 for the interaction of the core and valence particle with the target in terms of their phase-shifts

$$\chi = -\frac{1}{\hbar v} \int_{-\infty}^{\infty} dZ V(R) . \quad (9)$$

In the weak interaction limit, or perturbation limit, the phase-shifts are very small so that

$$\begin{aligned} S_c(b_c) S_v(b_v) &= \exp[i(\chi_c + \chi_v)] \simeq 1 + i\chi_c + i\chi_v \\ &= 1 - \frac{i}{\hbar v} \int V_{cT}(\mathbf{r}_c) dz_c - \frac{i}{\hbar v} \int V_{vT}(\mathbf{r}_v) dz_v. \end{aligned} \quad (10)$$

The factor 1 does not contribute to the breakup. Thus, inserting the result above in eq. 4, we obtain

$$A_{(\text{PWBA})} \simeq \frac{1}{i\hbar v} \int d^3r_c d^3r_v \phi_f^*(\mathbf{r}) \phi_i(\mathbf{r}) [V_{cT}(\mathbf{r}_c) + V_{vT}(\mathbf{r}_v)] \exp[i(\mathbf{q}_c \cdot \mathbf{r}_c + \mathbf{q}_v \cdot \mathbf{r}_v)], \quad (11)$$

where the integrals over z_c and z_v in eq. 10 were absorbed back to the integrals over \mathbf{r}_c and \mathbf{r}_v after use of the delta-function $\delta(z_c + z_v)$. The above equation is nothing more than the plane-wave Born-approximation (PWBA) amplitude. However, absorption is not treated properly. For small values of \mathbf{r}_c and \mathbf{r}_v the phase-shifts are not small and the approximation used in eq. 10 fails. A better approximation is to assume that for small distances, where absorption is important, $S_c(b_c) S_v(b_v) \simeq S(b)$, where the right-hand side is the S -matrix for the projectile scattering as a whole on the target. Using the coordinates \mathbf{r} and \mathbf{R} , and defining $U_{int}(\mathbf{r}, \mathbf{R}) = V_{cT}(\mathbf{r}_c) + V_{vT}(\mathbf{r}_v)$, one gets

$$T_{(\text{DWBA})} = \hbar v A_{(\text{DWBA})} \simeq \int d^3r d^3R \phi_f^*(\mathbf{r}) \exp[i\mathbf{q} \cdot \mathbf{r}] \phi_i(\mathbf{r}) U_{int}(\mathbf{r}, \mathbf{R}) S(b) \exp[i\mathbf{Q} \cdot \mathbf{R}] . \quad (12)$$

In elastic scattering, or excitation of collective modes (e.g. giant resonances), the momentum transfer to the intrinsic coordinates can be neglected and the equation above can be written as

$$T_{(\text{DWBA})} = \langle \chi^{(-)}(\mathbf{R}) \phi_c(\mathbf{r}) | U_{\text{int}}(\mathbf{r}, \mathbf{R}) | \chi^{(+)}(\mathbf{R}) \phi_i(\mathbf{r}) \rangle , \quad (13)$$

which has the known form of the DWBA T-matrix. The scattering phase space now only depends on the center of mass momentum transfer \mathbf{Q} . When the center of mass scattering waves are represented by eikonal wavefunctions, one has

$$\chi^{(-)*}(\mathbf{R}) \chi^{(+)}(\mathbf{R}) \simeq S(b) \exp[i\mathbf{Q} \cdot \mathbf{R}] . \quad (14)$$

This shows that the PWBA and the DWBA are perturbative expansions of the diffraction dissociation formula 4.

In DWBA (or in the eikonal approximation, eq. 14), b does not have the classical meaning of an impact parameter. To obtain the semiclassical limit one goes one step further. By using eq. 12 and assuming that R depends on time so that $R = (\mathbf{b}, z = vt)$, the semiclassical scattering amplitude is given by $A_{(\text{semiclass})}^{(i \rightarrow f)}(b) = \int d^2b a_{(\text{semiclass})}^{(i \rightarrow f)}(b) \exp(i\mathbf{Q} \cdot \mathbf{b})$, where

$$a_{(\text{semiclass})}^{(i \rightarrow f)}(b) = \frac{1}{i\hbar} S(b) \int dt d^3r \exp(i\omega_{if} t) \phi_f^*(\mathbf{r}) U_{\text{int}}(\mathbf{r}, t) \phi_i(\mathbf{r}) , \quad (15)$$

where eq. 1 was used ($Q_z Z = \omega_{if} t$).

The semiclassical probability for the transition ($i \rightarrow f$) is obtained from the above equation after integration over \mathbf{Q} . One gets $P_{(\text{semiclass})}^{(i \rightarrow f)}(b) = \left| a_{(\text{semiclass})}^{(i \rightarrow f)}(b) \right|^2$, with b having now the explicit meaning of an impact parameter. Thus, $a_{(\text{semiclass})}^{(i \rightarrow f)}(b)$, is the semiclassical excitation amplitude. Equation 15 is well-known (for example in Coulomb excitation at low energies) except that the factor $S(b)$ is usually set to one. In high energy collisions it is crucial to keep this factor, as it accounts for refraction and absorption at small impact parameters: $|S(b)|^2 = \exp[2\chi^{(\text{imag})}]$, where $\chi^{(\text{imag})}$ is calculated with the imaginary part of the optical potential. The derivation of the DWBA and semiclassical limits of eikonal methods can be easily extended to higher-orders in the perturbation V . The eikonal method includes all terms of the perturbation series in the sudden-collision limit.

IV. ROLE OF ABSORPTION AND OF LORENTZ BOOSTS

At this point it is interesting to consider the calculation performed by Feshbach and Zabek [9]. In that work, eq. 15, or its equivalent PWBA form, eq. 11, without a proper

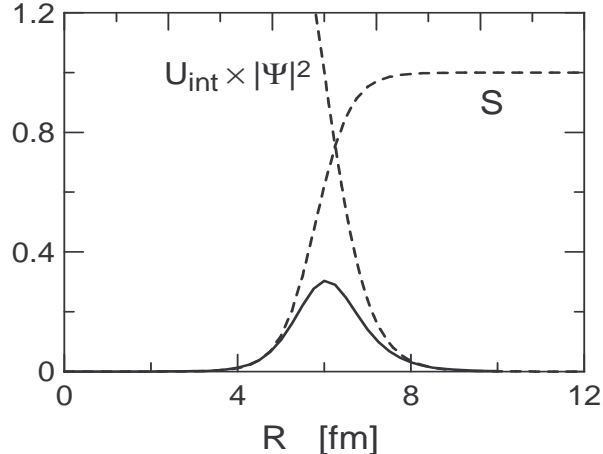


FIG. 1: Schematic diagram showing how the product of the S-matrix and the interaction potential (weighted by the wavefunction) would limit the cross section to grazing impact parameters.

account of the strong absorption at small impact parameters (described in eq. 15 by $S(b)$), was used to calculate the total cross section for emission of a correlated nucleon pair in peripheral collisions with heavy ions. Also, interactions without imaginary parts were used. As a consequence, they found extremely large cross sections; ~ 1 barn for $^{16}\text{O}+^{16}\text{O}$ collisions at energies ~ 1 GeV/nucleon. This is certainly inconsistent with perturbation theory. As seen schematically in figure 1, the product of the S -matrix and the interaction potential implies that the reaction occurs in a narrow region at “grazing” impact parameters. The width of this region is approximately $\Delta \simeq 1 - 2$ fm. The cross section might be written as $\sigma \simeq 2\pi\Delta (R_P + R_T) P$, where P is the average probability for this reaction to occur within the distance Δ . For light nuclei $2\pi\Delta (R_P + R_T) \simeq 300 - 600$ mb. Thus, the probability P violates unitarity (perturbation theory is invalid) if cross sections of the order of 1 b are obtained.

Ref. [9] also introduced relativistic corrections to the nuclear potential. This relativistic property is most easily seen within a folding potential model for a nucleon-nucleus collision:

$$V(\mathbf{r}) = \int dr'^3 \rho_T(\mathbf{r}') v_{NN}(\mathbf{r} - \mathbf{r}'), \quad (16)$$

where $\rho_T(\mathbf{r}')$ is the nuclear density of the target. In the frame of reference of the projectile, the density of the target looks contracted and particle number conservation leads to the relativistic modification of eq. 16 so that $\rho_T(\mathbf{r}') \rightarrow \gamma\rho_T(\mathbf{r}'_{\perp}, \gamma z')$, where \mathbf{r}'_{\perp} is the transverse

component of \mathbf{r}' and $\gamma = (1 - v^2/c^2)^{-1/2}$ is the Lorentz contraction factor, with v equal to the relative velocity of projectile and target. But the number of nucleons as seen by the target (or projectile) per unit area remains the same. In other words, a change of variables $z'' = \gamma z'$ in the integral of eq. 16 seems to restore the same eq. 16. However, this change of variables also modifies the nucleon-nucleon interaction v_{NN} . Thus, relativity introduces non-trivial effects in a potential model description of nucleus-nucleus scattering at high energies. Colloquially speaking, nucleus-nucleus scattering at high energies is not simply an incoherent sequence of nucleon-nucleon collisions. Since the nucleons are confined within a box (inside the nucleus), Lorentz contraction induces a collective effect: in the extreme limit $\gamma \rightarrow \infty$ all nucleons would interact at once with the projectile. This is often neglected in pure geometrical (Glauber model) descriptions of nucleus-nucleus collisions at high energies, as it is assumed that the nucleons inside “firtubes” scatter independently.

Assuming that the nucleon-nucleon interaction is of very short range so that the approximation $v_{NN}(\mathbf{r} - \mathbf{r}') = J_0 \delta(\mathbf{r} - \mathbf{r}')$ can be used, one sees from eq. 16 that $V(\mathbf{r})$, the interaction that a nucleon in the projectile has with the target nucleus, also has similar transformation properties as the density: $V(\mathbf{r}) \rightarrow \gamma V(\mathbf{r}_\perp, \gamma z)$, i.e. $V(\mathbf{r})$ transforms as the time-component of a four-vector. In this situation, the Lorentz contraction has no effect whatsoever in the diffraction dissociation amplitudes, described in the previous sections within the eikonal approximation. This is because a change of variables $Z' = \gamma Z$ in the eikonal phases leads to the same result as in the non-relativistic case, as can be easily checked from eq. 9. Of course, the delta-function approximation for the nucleon nucleon interaction means that nucleons will scatter at once, and Lorentz contraction does not introduce any additional collective effect. This is not the case for realistic interactions with finite range.

V. EMISSION OF CORRELATED PAIRS IN PERIPHERAL REACTIONS

Lets us now consider the emission of correlated pairs in peripheral collisions. The projectile is now a three-body system, with notation for the coordinates as shown in figure 2. Following the same arguments used in section 2, the wavefunction of a three-body projectile

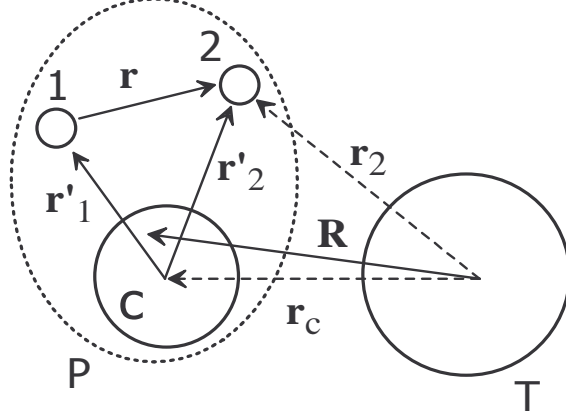


FIG. 2: Coordinates used in text for the three-body projectile interacting with the target. the coordinate \mathbf{r}_1 is not shown for simplicity.

in the initial and final states is given by

$$\begin{aligned}\Psi_i &= \phi_i(\mathbf{r}_1, \mathbf{r}_2) \exp [i(\mathbf{K}_c \cdot \mathbf{r}_c + \mathbf{k}_1 \cdot \mathbf{r}_1 + \mathbf{k}_2 \cdot \mathbf{r}_2)] \\ \Psi_f &= \phi_f(\mathbf{r}_1, \mathbf{r}_2) S_c(b_c) S_1(b_1) S_2(b_2) \exp [i(\mathbf{K}'_c \cdot \mathbf{r}_c + \mathbf{k}'_1 \cdot \mathbf{r}_1 + \mathbf{k}'_2 \cdot \mathbf{r}_2)] ,\end{aligned}\quad (17)$$

where now $\phi_{i,f}(\mathbf{r}_1, \mathbf{r}_2)$ are the initial and final intrinsic wavefunctions of the correlated nucleon-nucleon pair as a function of their intrinsic coordinates $\mathbf{r}_1, \mathbf{r}_2$. Assuming that the nucleon mass is much smaller than that of the core, one can replace $\mathbf{r}_c \simeq \mathbf{R}$, where \mathbf{R} is the center of mass of the projectile. A relation similar to eq. 8 can be obtained for the cross section for the energy absorption by a correlated pair (when final state interactions are neglected):

$$\begin{aligned}d\sigma &= \frac{d^3q_1 d^3q_2 d^2Q}{(2\pi)^8} \left| \int d^3r_1 d^3r_2 d^2b \phi_f^*(\mathbf{r}_1, \mathbf{r}_2) \phi_i(\mathbf{r}_1, \mathbf{r}_2) \right. \\ &\quad \left. \times S(b) S_1(b_1) S_2(b_2) \exp [i(\mathbf{q}_1 \cdot \mathbf{r}_1 + \mathbf{q}_2 \cdot \mathbf{r}_2 + \mathbf{Q} \cdot \mathbf{b})] \right|^2 ,\end{aligned}\quad (18)$$

where $\mathbf{Q} = \mathbf{K}'_c - \mathbf{K}_c$. If the intrinsic nucleon coordinates are denoted by $\mathbf{r}'_i = \mathbf{r}_i - \mathbf{R}$, one has $b_i = \sqrt{b^2 + r_i^2 \sin^2 \theta_i + 2r_i \sin \theta_i b \cos(\phi - \phi_i)}$.

The above relation can be used for the emission of the nucleon pair. Neglecting final state interactions and assuming that the core is not observed (i.e. integrating over \mathbf{Q}), one gets

$$d\sigma = \frac{d^3q_1 d^3q_2}{(2\pi)^6} \int d^2b |S(b)|^2 \left| \int d^3r_1 d^3r_2 \phi_i(\mathbf{r}_1, \mathbf{r}_2) S_1(b_1) S_2(b_2) \exp [i(\mathbf{q}_1 \cdot \mathbf{r}_1 + \mathbf{q}_2 \cdot \mathbf{r}_2)] \right|^2 .\quad (19)$$

In order to proceed we need a model wavefunction for the correlated pair, $\phi_i(\mathbf{r}_n, \mathbf{r}_{n'})$. The wavefunction used will have the form

$$\phi_i(\mathbf{r}_1, \mathbf{r}_2) = \phi_\alpha(\mathbf{r}_1) \phi_\beta(\mathbf{r}_2) f_{\text{corr}}(\mathbf{r}), \quad (20)$$

where $\mathbf{r} = \mathbf{r}_1 - \mathbf{r}_2$, $\phi_\alpha(\mathbf{r}) = \phi_{nljm}(\mathbf{r})$ are single particle wavefunctions with quantum numbers $\alpha = nljm$, and $f(\mathbf{r}, \mathbf{r}_c)$ is a function for the nucleon pair distance \mathbf{r} , which also depends on a two-particle correlation parameter \mathbf{r}_c so that $f(\mathbf{r}, \mathbf{r}_c) \rightarrow 1$ as $\mathbf{r}_c \rightarrow 0$. The effective correlation function $f(\mathbf{r}, \mathbf{r}_c)$, the so-called Jastrow factor [27], is a statistical average of the Pauli correlation function [26] and the correlation function for the dynamical short-range (e.g., hard core) correlation.

As argued in ref. [28], the true ground-state wave function of the nucleus containing correlations coincide with the independent particle, or Hartree-Fock wavefunction, for interparticle distances $r \geq r_{\text{heal}}$, where $r_{\text{heal}} \simeq 1$ fm is the so-called ‘‘healing distance’’. This behavior is a consequence of the constraints imposed by the Pauli principle. Nucleons are kept apart at short-distances, while for distances beyond several K_F^{-1} ’s there is little effect. Consequently, nucleon-nucleon collisions at short distances are rare in nuclear matter, and because the strongest part of the interaction is at short distances, the effective force between the nucleons is much less than in free space. For example, if a nucleon in ^{16}O felt the cumulative sum of 16 nucleon-nucleon potentials, it would feel a potential of ~ 1400 MeV; yet empirically it is known that the effective potential felt by the nucleon in the middle of the nucleus is only ~ 40 -50 MeV deep.

Although, in general, the correlation function $f(\mathbf{r}, \mathbf{r}_c)$ may depend on the isospin and spin quantum numbers of the two-body channel, we will assume, for simplicity, that it is a plain, state independent Jastrow factor [27]. The effects of nucleon-nucleon correlations in nucleus-nucleus collisions have also been studied in several works. For example, in ref. [29] short-range correlations were shown to play an important role in nucleon-nucleus collisions at intermediate and high energies.

The two-particle correlation distance, \mathbf{r}_c , is a combination of four contributions [29]

$$r_c = r_{\text{Pauli}} + r_{\text{SRD}} + r_{\text{PSR}} + r_{\text{CM}}, \quad (21)$$

where r_{Pauli} is due to Pauli exclusion-principle correlations, r_{SRD} is related to short-range dynamical correlations, r_{PSR} is due to a combination of the Pauli and the short-range dy-

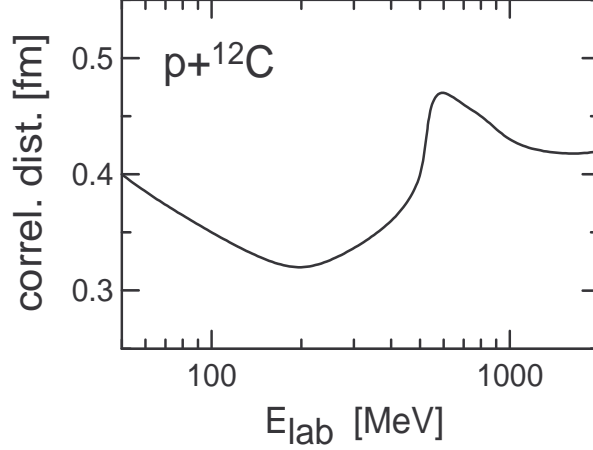


FIG. 3: Dependence of the short-range correlation distance, r_c , on the proton energy in the reaction $p + {}^{12}\text{C}$.

namical term, and r_{CM} is due to center-of-mass correlations [30]. An approximate set of expressions for each of these terms is given by

$$\begin{aligned}
 r_{\text{Pauli}} &= \frac{1}{2} \left(1 - \frac{5}{A} + \frac{4}{A^2} \right) \frac{3\pi}{10K_F} \frac{1}{1 + \frac{8}{5}BK_F^2}, \\
 r_{\text{SRD}} &= \frac{1}{2} \left(1 - \frac{2}{A} + \frac{1}{A^2} \right) \sqrt{\pi} \frac{b^3}{b^2 + 8B}, \\
 r_{\text{PSR}} &= \frac{1}{2} \left(1 - \frac{5}{A} + \frac{4}{A^2} \right) \frac{3\pi}{10} \left(K_F^2 + \frac{5}{b^2} \right)^{-1/2} \left[1 + 8B \left(\frac{K_F^2}{5} + \frac{1}{b^2} \right) \right]^{-1} \\
 r_{\text{CM}} &= \left(1 - \frac{2}{A} + \frac{1}{A^2} \right) l_c,
 \end{aligned} \tag{22}$$

where A and $K_F = (1.5\pi^2\rho)^{1/3} \simeq 1.36 \text{ fm}^{-1}$ are the target number and the Fermi momentum of the target nucleus, respectively. b is a short-range dynamical correlation, $b \simeq 0.4 \text{ fm}$, B is the finite-range parameter of the nucleon-nucleon elastic t -matrix, $B \simeq 0.62 \text{ fm}^2$ (for collisions around 200 MeV/nucleon), and l_c is the effective ‘‘correlation length’’, $l_c \simeq 1.3 A^{-5/6} \text{ fm}$. For proton+ ${}^{12}\text{C}$ collisions at 200 MeV/nucleon this set of parameters yields, $r_{\text{Pauli}} \simeq 0.3 \text{ fm}$, $r_{\text{SRD}} \simeq 0.01 \text{ fm}$, $r_{\text{PSR}} \simeq 0.0016 \text{ fm}$, $r_{\text{CM}} \simeq 0.18 \text{ fm}$, and $r_c \simeq 0.5 \text{ fm}$. This in fact overestimates the correlation distance. A more detailed calculation, using the parameters B , b and l_c from ref. [29] shows that r_c has an appreciable dependence on the collision energy, as shown in figure 3 for protons incident on ${}^{12}\text{C}$. Thus, in nuclear reactions, r_c can vary substantially with the collision energy and with mass numbers.

The estimates done above show that the main contribution to the correlation distance

arises from the Pauli principle. Let us assume a correlation function of the form

$$f_{\text{corr}}(r) = 1 - \exp \left[-\frac{(\mathbf{r}_1 - \mathbf{r}_2)^2}{r_c^2} \right]. \quad (23)$$

This correlation function implies that the pair wavefunction decreases for small relative distances, $r = |\mathbf{r}_1 - \mathbf{r}_2| \lesssim r_c$. The correlation function $f_{\text{corr}}(r)$ goes to one for large values of r and to zero for $r \rightarrow 0$. In nuclear structure calculations, the effect of correlation, introduced by the function $f_{\text{corr}}(r)$, becomes large when the correlation distance parameter r_c becomes large, and vice versa. Here, only the effects of short-range correlations are studied and it would be manifest in momentum distributions of highly energetic nucleons, as discussed in the introduction, and explicitly shown in the next section.

Inserting eqs. 20 and 23 in eq. 19 and integrating over the pair momenta, one gets

$$\sigma_{\text{corr}} = \sigma_{\text{indep}} - \sigma_{\text{SR}} \quad (24)$$

where

$$\begin{aligned} \sigma_{\text{indep}} &= \frac{(C^2S)_{lj} (C^2S)_{l'j'}}{(2j+1)(2j'+1)} \sum_{m, m'} \int d^2b |S(b)|^2 \int d^3r_1 |\phi_{nljm}(\mathbf{r}_1) S_1(b_1)|^2 \\ &\times \int d^3r_2 |\phi_{n'l'j'm'}(\mathbf{r}_2) S_2(b_2)|^2 \end{aligned} \quad (25)$$

is the cross section for independent scattering of each nucleon to continuum states, and

$$\begin{aligned} \sigma_{\text{SR}} &= \frac{(C^2S)_{lj} (C^2S)_{l'j'}}{(2j+1)(2j'+1)} \sum_{m, m'} \int d^2b |S(b)|^2 \\ &\times \int d^3r_1 d^3r_2 \left| \phi_{nljm}(\mathbf{r}_1) S_1(b_1) \phi_{n'l'j'm'}(\mathbf{r}_2) S_2(b_2) \exp \left(-\frac{r^2}{r_c^2} \right) \right|^2. \end{aligned} \quad (26)$$

These cross sections have been averaged over the initial magnetic quantum numbers of the nucleons. From eq. 25 we see that the probability to remove an uncorrelated nucleon, with quantum numbers $nljm$, is given by $\int d^3r_1 |\phi_{nljm}(\mathbf{r}_1) S_1(b_1)|^2$.

The spectroscopic factors in eqs. 24 and 25 have a complex dependence on the angular momenta of the nucleon pair. The correlations arising from angular momentum coupling have been studied in ref. [32]. Here we will assume a simple combinatorics so that $(C^2S)_{lj} = n(n-1)/2$, where n is the number of nucleons in the valence shell.

We see from the equations above that the cross section for the emission of a correlated pair is smaller than that for the emission of independent particles, since $\sigma_{\text{SR}} > 0$. In fact,

most part of the integrands will be the same, leaving out only but the small cross sectional area of the pair, which is approximately equal to $\mathcal{N}r_c^2$, where \mathcal{N} is a number which cannot be much different one. Conservative estimates (using $r_c = 0.3 - 1$ fm), implies that the cross section for emission of a correlated pair could not exceed 100 mb by much, in contrast to the results obtained in refs. [9, 10]. We will show this for specific reactions in the following section.

VI. RESULTS AND DISCUSSIONS

The numerical calculations have been carried out for the systems $^{12}\text{C}+^{12}\text{C}$ at 250 MeV/nucleon and $^{11}\text{Li}+^9\text{Be}$ at 287 MeV/nucleon. In both cases, there are some experimental data available for two-nucleon removal. This also allows for the study of the influence of a halo wavefunction (^{11}Li) in the results. The wavefunctions were calculated by using a Woods-Saxon potential with a spin-orbit and Coulomb potential,

$$V(r) = U_r(r) + U_s(r) + U_C(r), \quad (27)$$

where

$$U_r(r) = V_r(1 + e^{\rho_r})^{-1}, \quad U_s(r) = V_s(\mathbf{1} \cdot \mathbf{s}) \frac{(2 \text{ fm}^2)}{r} \frac{d}{dr} (1 + e^{\rho_s})^{-1}, \quad (28)$$

$U_C(r)$ is the potential for a uniformly charged sphere with charge $Z - 1$ (Z , for neutrons) and radius R_C , and $\rho_i = (r - R_i)/a_i$.

For protons in the $1p_{3/2}$ orbital of ^{12}C the separation energy is 15.96 MeV (the two-proton separation energy is 27.18 MeV), which can be reproduced with the parameters $V_r = -57.41$ MeV, $V_s = -6.0$ MeV, $R_r = R_C = R_s = 3.011$ fm, $a_r = 0.52$ fm and $a_s = 0.65$ fm.

The reactions and structure of the two-neutron halo nucleus ^{11}Li have attracted much interest. It is a Borromean system in the sense that although the three-body system, consisting of ^9Li and two neutrons, forms a bound state, none of the possible two-body subsystems have bound states. Hence the stability of ^{11}Li is brought about by the interplay of the core-neutron and the neutron-neutron interactions, which must lead to a strongly correlated wave function with the two neutrons spatially close together. For the calculation here we will approximate the ^{11}Li ground state by an inert ^9Li core coupled to a neutron pair in a $(2s1/2)^2$ state, although the most probable configuration is an admixture of neutron pairs in

$(2s1/2)^2$, $(1p1/2)^2$, and $(1d5/2)^2$ states [33, 34]. However, the former assumption allows for a simpler calculation of the correlated-pair emission. The potential parameters are adjusted to obtain the single-particle wave functions, reproducing the effective neutron separation energies. The two-neutron separation energy is 0.3 MeV. From the systematics in Fig. 6 of [35], the estimated ^{10}Li average excitation energies is 0.2 MeV for the single-particle state. Taking this value for two-neutron coupling to the ^9Li core, one arrives at an effective neutron-separation energy of 0.5 MeV. This binding energy for the $n+^{10}\text{Li}$ system can be reproduced with the potential parameters $V_r = -42.93$ MeV, $V_s = -6.0$ MeV, $R_r = R_C = R_s = 3.25$ fm and $a_r = a_s = 0.65$ fm.

The single-particle wavefunctions obtained in this way were used in eq. 19 to calculate the momentum distributions of the correlated pair. Using the correlation factor given by eq. 23, the cross sections factorize, similarly to eq. 24. The first term, $d\sigma_{\text{indep}}$, is easy to integrate. The second term requires more effort, because the integrand is entangled due to the second term of eq. 23. This integral can be performed more easily if the S-matrices and the single-particle wavefunctions are expanded in terms of gaussian functions, as explained in the appendix of ref. [34]. Using this method, many integrals can be performed analytically and are replaced by finite sums ($\simeq 40$ terms) of fewer integrals.

The S-matrices (and optical potentials) were calculated by using the “ $t\text{-}\rho\rho$ ” interaction, as described in refs. [29, 31]. This is the same approximation used in ref. [5].

In heavy ion physics it is common to define a correlation function by means of

$$C(\mathbf{q}_1, \mathbf{q}_2) = \left(\frac{d\sigma}{d^3q_1 d^3q_2} \right) / \left(\frac{1}{\sigma} \frac{d\sigma}{d^3q_1} \frac{d\sigma}{d^3q_2} \right), \quad (29)$$

where the cross sections in the denominator are for the emission of a single nucleon. An accurate measurement of r_c requires the measurement of this correlation function for back-to-back (or nearly) pair emission. Until now, heavy ion data refers mainly to small relative momentum transfers. Data would only be interesting for the present purposes if the triggering conditions were changed and if special attention was paid to back-to-back emission. In the present work, $d\sigma/dq_1 dq_2$, instead of $C(\mathbf{q}_1, \mathbf{q}_2)$, will be used for the study of emission of correlated nucleons.

In figure 4 contour plots for $d\sigma/dq_1 dq_2$ are presented for the collision $^{12}\text{C}+^{12}\text{C}$ at 250 MeV/nucleon and $^{11}\text{Li}+^9\text{Be}$ at 287 MeV/nucleon, as a function of $p_1 = \hbar q_1$ and $p_2 = \hbar q_2$. The nucleons are assumed to be emitted back-to-back, the nucleon 1 at 0° and nucleon 2

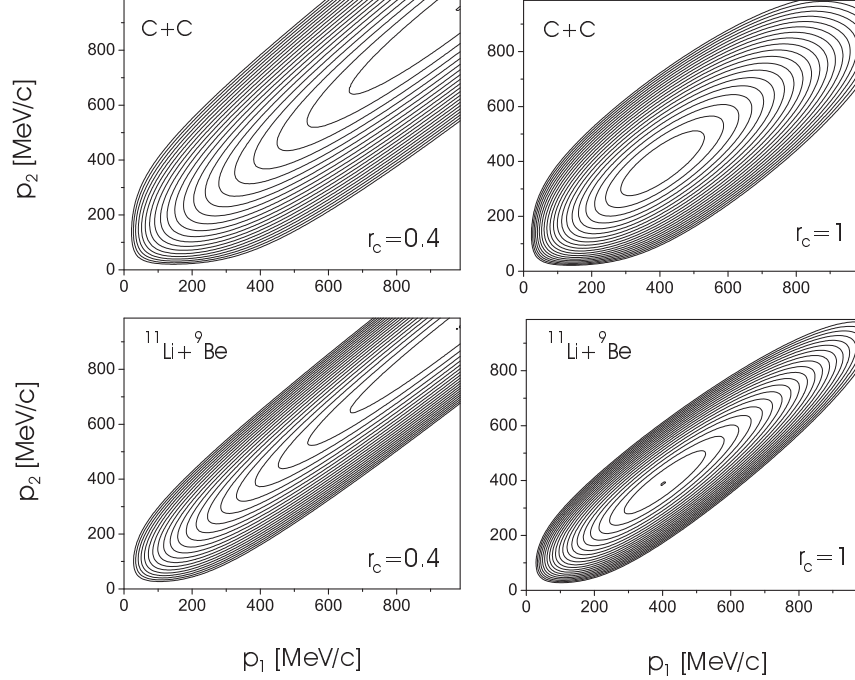


FIG. 4: Contour plots for $d\sigma/dq_1dq_2$ for the collision $^{12}\text{C}+^{12}\text{C}$ at 250 MeV/nucleon (upper panels) and $^{11}\text{Li}+^9\text{Be}$ at 287 MeV/nucleon (lower panels), as a function of $p_1 = \hbar q_1$ and $p_2 = \hbar q_2$. The left (right) panels are for $r_c = 0.4$ (1) fm.

at 180° with respect to the beam axis, respectively. The upper panels are for the C+C collision, while the lower panels are for the Li+Be collisions. The left (right) panels are for $r_c = 0.4$ fm ($r_c = 1$ fm). One notices a strong correlation between the nucleon momenta, resulting from the phonon relationship, eq. 1. The effect of the phonon dispersion relation is to produce a ridge in the cross section.

To illustrate better this effect, let us use the DWBA approximation as in eq. 12, so that, instead of the integrals in eq. 19, we need now to calculate

$$T_{(\text{DWBA})} = \int d^3r_1 d^3r_2 \phi_i(\mathbf{r}_1, \mathbf{r}_2) [V_1(\mathbf{r}_1) + V_2(\mathbf{r}_2)] \exp[i(\mathbf{q}_1 \cdot \mathbf{r}_1 + \mathbf{q}_2 \cdot \mathbf{r}_2)]. \quad (30)$$

Let us assume that the potentials $V_{1,2}$ are given by Gaussian functions, i.e. $V_{1,2} = V_{1,2}^{(0)} \exp(-r_{1,2}^2/\lambda^2)$ and similarly for the wavefunctions, i.e. $\phi_{\alpha,\beta} = N \exp(-r_{1,2}^2/\Delta^2)$. In this case it is straightforward to perform analytically all the integrals in eq. 30. If one further assumes that the correlation distance, r_c , is much smaller than the dimensions of the

uncorrelated wavefunctions and of the potential, i.e. if $r_c \ll \Delta, \lambda$, one gets

$$T_{(\text{DWBA})} = \left(V_1^{(0)} + V_2^{(0)} \right) \frac{\left(\pi N^2 r_c \Delta / \sqrt{\mathcal{A}} \right)^3}{8} \left[\exp \left(-\frac{q_1^2 r_c^2}{4} \right) + \exp \left(-\frac{q_2^2 r_c^2}{4} \right) \right] \\ \times \exp \left[-\frac{\Delta^2}{16\mathcal{A}} |\mathbf{q}_{1\perp} + \mathbf{q}_{2\perp}|^2 \right] \exp \left[-\frac{\Delta^2}{16\mathcal{A}} \left(q_{1z} + q_{2z} - \frac{\omega}{v} \right)^2 \right],$$

where B is the separation energy of the pair and $\mathcal{A} = (1 + \Delta/\lambda)/2$. Therefore, the cross section is given by

$$\frac{d\sigma}{dq_1 dq_2} \propto q_1^2 q_2^2 \exp \left[-\frac{\Delta^2}{8\mathcal{A}} \left(q_{1z} + q_{2z} - \frac{\omega}{v} \right)^2 \right] \\ \times \exp \left[-\frac{\Delta^2}{8\mathcal{A}} |\mathbf{q}_{1\perp} + \mathbf{q}_{2\perp}|^2 \right] \left[\exp \left(-\frac{q_1^2 r_c^2}{4} \right) + \exp \left(-\frac{q_2^2 r_c^2}{4} \right) \right]^2. \quad (31)$$

Now we can easily understand the physics in figure 4 by identifying the terms of the above equation. The first term is due to conservation of the momentum along the beam direction, which yields the dispersion relation, eq. 1. Note that in the derivation of eq. 19 it was assumed that the core recoils with the same momentum, i.e. $Q_Z \simeq \omega/v = -(q_{1z} + q_{2z})$. The second term is due to elastic scattering of the pair on the target in the direction transverse to the beam. In eq. 31 both the first and the second terms imply that the momentum distribution of correlated pair is such that $q_1 + q_2 = \omega/v$, i.e. $q_1 \simeq -q_2$, as expected for small r_c . Also according to these terms, the distribution is smeared by the range of the independent wavefunctions of the pair, i.e. $\langle q_{1,2}^2 \rangle \simeq 1/\Delta^2$. However, the last term implies a smearing, or spreading, of the momentum distribution by a much larger factor (assuming $r_c \ll \Delta$), i.e. $\langle q_{1,2}^2 \rangle \simeq 1/r_c^2$. This explains all physics presented in figure 4. The second exponential term in eq. 31 plays no role in the results presented in figure 4, since it is identical to one.

As discussed above, the location of the ridges in figure 4 is a kinematical property of the phonon absorption mechanism, which is independent of the collision energy. Thus, it should be observable in intermediate energy collisions ($E_{lab} \simeq 100$ MeV/nucleon), as well as in relativistic collisions. One also observes that the momentum distributions are narrower for correlated-pair emission from a halo nucleus. This is due to the low binding energy, which yields an extended wavefunction of the nucleons in the halo. This is also seen from the first exponential term of eq. 31, since the two-proton separation energy for ^{12}C is 27.16 MeV, while the two-neutron separation energy is 0.3 MeV. The effective value of Δ is much smaller

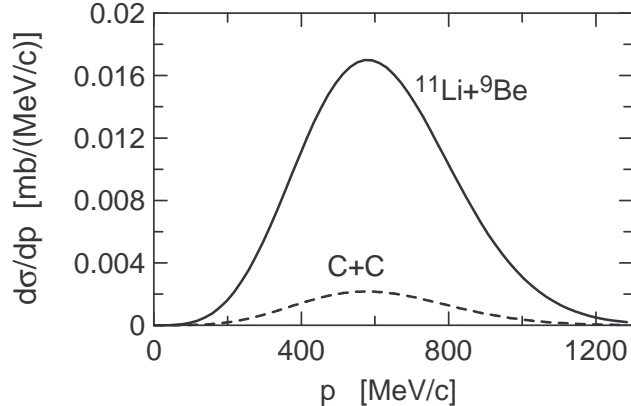


FIG. 5: Singles spectra for the momentum distribution of a nucleon due to the correlated-pair mechanism.

for the first case, leading to a larger spreading of the momentum distributions. However, the last term in eq. 31 is still the dominant one leading to a small overall effect on the momentum distribution, as shown next.

It would be interesting to try to observe the contribution of the emission of correlated pairs in singles spectra. This can be obtained by integrating $d\sigma/dq_1dq_2$ over one of the nucleon momentum. This is shown in figure 5 for C+C and Li+Be collisions, using $r_c = 0.7$ fm. One observes that the peak in the singles spectra occurs at $p \simeq \hbar/r_c$, as expected from the arguments presented above. This should be visible in the spectra of nucleons from knockout reactions as a bump at high nucleon momenta. The position of the bump would be a direct reading of the short-range correlation distance. Notice, however, that such a bump could not be noticeable because it is superposed to a large background of knockout nucleons from stripping reactions. Only by doing a measurement of back-to-back pair emission, this signature of short-range pair-correlations could be assessed.

Cross sections for nucleon knockout reactions with heavy ions, at intermediate energies and in inverse kinematics, have become a specific and quantitative tool for studying single-particle occupancies and correlation effects in the nuclear shell model [5]. The measured partial cross sections to individual final levels provide spectroscopic factors for the individual angular-momentum components j . Let us now compare the magnitude of the total cross section for the knockout of correlated pairs arising from short-range correlations with that of stripping and diffraction of a single nucleon. The former cross sections can be calculated

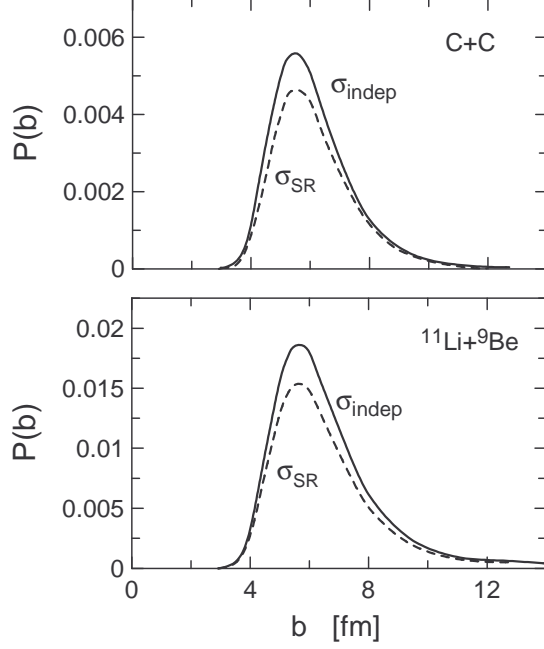


FIG. 6: Probabilities for two-nucleon removal for $^{12}\text{C}+^{12}\text{C}$ at 250 MeV/nucleon (upper panel) and $^{11}\text{Li}+^9\text{Be}$ at 287 MeV/nucleon (lower panel), as a function of the impact parameter in the collision.

from eqs. 24, 25 and 26. It is illustrative to plot the probabilities for the emission of uncorrelated pairs,

$$P_{\text{indep}}(b) = |S(b)|^2 \int d^3r_1 |\phi_1(\mathbf{r}_1) S_1(b_1)|^2 \int d^3r_2 |\phi_2(\mathbf{r}_2) S_2(b_2)|^2,$$

and the probabilities arising from the short-range correlation factor,

$$P_{\text{SR}}(b) = |S(b)|^2 \int d^3r_1 d^3r_2 \left| \phi_1(\mathbf{r}_1) S_1(b_1) \phi_2(\mathbf{r}_2) S_2(b_2) \exp\left(-\frac{r^2}{r_c^2}\right) \right|^2.$$

One sees from figure 6 that the knockout probabilities for the two-nucleon removal are indeed very small. Thus, one justifies the use of the DWBA approximation, eq. 30, which is useful to understand the results presented in figure 4, through the use of eq. 31. One also sees that $P_{\text{SR}}(b)$ is indeed always smaller than $P_{\text{indep}}(b)$, as discussed above. For the Li+Be case the probabilities for pair emission extend a bit further out in impact parameter due to the extended wavefunction of ^{11}Li . But the effect is hardly visible.

Assuming $r_c = 0.7$ fm, the cross sections for C+C at 250 MeV/nucleon are $\sigma_{\text{indep}} = 8.21$ mb and $\sigma_{\text{SR}} = 7.60$ mb, yielding $\sigma_{\text{corr}} = 0.61$ mb for the total cross section for the emission

of high-energy correlated pairs. The experimental value for two-proton knockout in this collision is 5.88 ± 9.70 mb. If one accepts the value of 6 mb for this cross section, one sees that the short-range correlations contribute to a small factor, of the order of 10%, of the cross section for two-proton knockout. The same numbers for $^{11}\text{Li}+^9\text{Be}$ at 287 MeV/nucleon are $\sigma_{\text{indep}} = 26.43$ mb, $\sigma_{\text{SR}} = 22.32$ mb, and $\sigma_{\text{corr}} = 4.11$ mb. Note that these cross sections are much smaller than those obtained in refs. [9, 10]. For reasons which were explained in the paragraph preceding eq. 16, the results obtained here are much more reasonable. These cross sections are also much smaller than those for one-nucleon knockout reactions (see, e.g. ref. [5]). They are also only one of the contributions (i.e. only from diffraction dissociation) of the two-proton removal cross section. Another contribution (stripping) has not been considered here. Stripping would not contribute to back-to-back nucleon emission, with nearly zero total momentum of the pair.

In conclusion, we have shown that when a projectile reacts with a light nuclear target, the short-range correlations contribute to the emission of high-energy nucleons which can be visible in measurements of back-to-back emission of nucleon pairs. More experiments and also the development of a more complete reaction theory are interesting challenges. The theoretical results suggest that the pattern and absolute magnitudes of the partial cross sections will provide specific information on the detailed nature of the states involved. This is particularly important in the case of reactions involving neutron-rich and proton-rich nuclei, far from the stability valley, for which only nuclear reactions are presently capable of probing their internal structure. The results presented here will be valuable as a guide to extend these studies towards drip line nuclei and look for effects which cannot be probed in (e, e') scattering due to the lack of experimental facilities of electron scattering on drip line nuclei.

This work was supported by the U. S. Department of Energy under grant No. DE-FG02-04ER41338.

[1] R.J. Glauber, Lectures in theoretical physics, Vol. 1, Eds. W.E. Brittin and L.G. Dunham (Interscience, New York, 1959).

[2] T. Fujita and J. Hufner, Nucl. Phys A 343 (1980) 493.

- [3] J. Hufner and M.C. Nemes, *Phys. Rev. C* 23 (1981) 2538.
- [4] C.A. Bertulani, M. Hussein and G. Muenzenberg, “Physics of Radioactive Beams”, Nova Science, Hauppauge, NY, 2002.
- [5] P. G. Hansen and J. A. Tostevin, *Annu. Rev. Nucl. Part. Sci.* 53, 219 (2003).
- [6] C.A. Bertulani and G. Baur, *Phys. Reports* 163 (1988) 299.
- [7] T. Glasmacher, *Annu. Rev. Nucl. Part. Sci.* 48, 1 (1998).
- [8] C.A. Bertulani and V. Ponomarev, *Phys. Reports* 321 (1999) 139.
- [9] H. Feshbach and M. Zabeck, *Ann. of Phys.* 107 (1977) 110.
- [10] H. Feshbach, *Prog. Part. Nucl. Phys.* 4 (1980) 532.
- [11] G.E. Brown and P.A. Deutchman, Workshop on High resolution heavy ion physics at $E/A=20$ -100 MeV, Saclay, May 31-June 2, 1978, p. 212
- [12] N.S.P. King et al., *Phys. Lett. B*17S (1986) 279
- [13] L.W. Townsend and P.A. Deutchman, *Nucl. Phys. A*355 (1981) 505;
- [14] L.W. Townsend, P.A. Deutchman, R.L. Madigan and J.W. Norbury, *Nucl. Phys. A*415 (1984) 520;
- [15] J.W. Norbury, P.A. Deutchman and L.W. Townsend, *Nucl. Phys. A*433 (1985) 691;
- [16] P.A. Deutchman, J.W. Norbury and L.W. Townsend, *Nucl. Phys. A*454 (1986) 733.
- [17] P. Chomaz, N. Francaria, *Phys. Reports* 252 (1995) 275.
- [18] C. Barbieri and W.H. Dickhoff, *Phys. Rev. C* 63, 034313 (2001).
- [19] C. Barbieri and W.H. Dickhoff, *Phys. Rev. C* 65, 064313 (2002).
- [20] C.A. Bertulani, L.F. Canto, R. Donangelo and J.O. Rasmussen, *Mod. Phys. Lett. A* 4, 1315 (1989).
- [21] F.S. Navarra and M.C. Nemes, *Phys. Rev. C* 43, R939 (1991).
- [22] D. Bazin, B. A. Brown, C. M. Campbell, J. A. Church, D. C. Dinca, J. Enders, A. Gade, T. Glasmacher, P. G. Hansen, W. F. Mueller, H. Olliver, B. C. Perry, B. M. Sherrill, J. R. Terry, and J. A. Tostevin, *Phys. Rev. Lett.* 91, 012501 (2002).
- [23] C.A. Bertulani and P. Danielewicz, “Introduction to Nuclear Reactions”, IOP Publishing, London, 2004, p. 419.
- [24] K. Hencken, H. Esbensen and G. Bertsch, *Phys. Rev. C*54, 3043 (1996).
- [25] M.H. MacGregor, A. R. Arndt, and R.M. Wright, *Phys. Rev.* 182, 1714 (1969).
- [26] A. Bohr and B. Mottelson, “Nuclear Structure”, Benjamin, New York, 1969, Vol.1.

- [27] R. Jastrow, Phys. Rev. 98, 1479 (1955).
- [28] L.C. Gomes, J.D. Walecka and V.F. Weisskopf, Ann. Phys. (New York) 3 (1958) 241.
- [29] L. Ray, Phys. Rev. C 20, 1859 (1979).
- [30] E. Boridy and H. Feshbach, Ann. Phys. (NY) 109, 468 (1977).
- [31] M.S. Hussein, R. Rego and C.A. Bertulani, Phys. Reports 201 (1991) 279.
- [32] J. A. Tostevin, G. Podolyák, B. A. Brown and P. G. Hansen, Phys. Rev. C 70, 064602 (2004).
- [33] H. Simon¹, D. Aleksandrov, T. Aumann, L. Axelsson, T. Baumann, M. J. G. Borge, L. V. Chulkov, R. Collatz, J. Cub, W. Dostal, B. Eberlein, Th. W. Elze, H. Emling, H. Geissel, A. Gruenschloss, M. Hellstrom, J. Holeczek, R. Holzmann, B. Jonson, J. V. Kratz, G. Kraus, R. Kulesa, Y. Leifels, A. Leistenschneider, T. Leth, I. Mukha, G. Muenzenberg, F. Nickel, T. Nilsson, G. Nyman, B. Petersen, M. Pfützner, A. Richter, K. Riisager, C. Scheidenberger, G. Schrieder, W. Schwab, M. H. Smedberg, J. Stroth, A. Surowiec, O. Tengblad, and M. V. Zhukov, Phys. Rev. Lett. 83, 496 (1999).
- [34] C.A. Bertulani and P.G. Hansen, Phys. Rev. C70, 034609 (2004).
- [35] P. G. Hansen, Nucl. Phys. A682, 310c (2001).